Precise determination of h/m_e using a rotating, superconducting ring

S. B. Felch,* J. Tate, B. Cabrera, and J. T. Anderson†
Physics Department, Stanford University, Stanford, California 94305
(Received 21 January 1985)

A precise determination of h/m_e (Planck's constant divided by the free-electron mass) using a rotating, superconducting ring is in progress. The measurement is based on flux quantization and the London moment—two manifestations of the macroscopic quantum nature of superconductivity. Here we report the first results from a precision, thin-film niobium ring. These data have a statistical error of 10 parts per million (ppm). A systematic error exists at the level of 2500 ppm, due to the presence of electric charge on the rotor. A model for the charge distribution is suggested and used to adjust the results and obtain a value of h/m_e. This work has determined h/m_e directly to an accuracy of 100 ppm, a higher level of precision than previously reported. Recent theoretical calculations have predicted a relativistic mass increase of 150 ppm for electrons in superconducting niobium, but the uncertainty in our final results prevented the clear identification of this effect.

THEORY

A precise determination of h/m_e (Planck's constant divided by the free-electron mass) is in progress at Stanford University and uses several of the remarkable, macroscopic quantum properties of the superconducting state. The nonrelativistic basis for the measurement can be understood by examining the Ginzburg-Landau supercurrent,

$$\mathbf{j}=-(e^*\hbar/2im^*)(\Psi^*\nabla\Psi-\Psi\nabla\Psi^*)-(e^{*2}/m^*c)\Psi^*\Psi\mathbf{A}\ , \tag{1}$$

where $-e$ is the charge on the electron, the mass m^* and charge e^* are equal to $2m$ and $2e$, respectively, and Ψ is the superconducting order parameter with phase ϕ, $\Psi=|\Psi|e^{i\phi}$. To include the effects of rotation, we transform the canonical momentum $m\mathbf{v}-e\mathbf{A}/c$ into the rotating frame by using the Galilean relation $\mathbf{v}'=\mathbf{v}-\boldsymbol{\omega}\times\mathbf{r}$. Now we can define an effective vector potential

$$\mathbf{A}_\omega=-(mc/e)\boldsymbol{\omega}\times\mathbf{r} \tag{2}$$

and obtain the Ginzburg-Landau equation in the rotating frame by replacing $\mathbf{A}$ with $\mathbf{A}+\mathbf{A}_\omega$ in Eq. (1). So,

$$\mathbf{j}=-(e\hbar/m)|\Psi|^2\nabla\phi-(2e^2/mc)|\Psi|^2(\mathbf{A}+\mathbf{A}_\omega)\ . \tag{3}$$

Finally, if we integrate around a closed path Γ contained within the superconducting ring, which rotates at an angular velocity ω, we obtain

$$(mc/e^2)\oint_\Gamma \mathbf{j}\cdot d\mathbf{l}/n_s = -n(hc/2e)-\int_{S_\Gamma}\mathbf{B}\cdot d\mathbf{S}+(2mc/e)\boldsymbol{\omega}\cdot\mathbf{S}_\Gamma\ , \tag{4}$$

where $n_s=2|\Psi|^2$ is the number density of superelectrons and S_Γ is the area bounded by Γ. As usual, we have required that Ψ be a single-valued function, forcing the integral of the gradient to be an integer multiple of 2π. For $\omega=0$, Eq. (4) is exactly the fluxoid quantization equation with $\Phi_0=hc/2e$, the flux quantum of superconductivity. For a fixed n we find the London moment relation—a continuously varying flux proportional to spin speed. Also, for a fixed ω only fluxoid values separated by an integral number of Φ_0 are allowed. If we assume the only source of $\mathbf{B}$ to be the supercurrent $\mathbf{j}$ [any constant background field will cancel in Eq. (5) below], then there exists a unique ω_n for each number of flux quanta n such that $\mathbf{j}=0$ and hence $\mathbf{B}=0$. Now from Eq. (4) we obtain the simple relation

$$h/m_e=4S\Delta\omega\ , \tag{5}$$

where $\Delta\omega=\omega_n-\omega_{n-1}$ is the angular velocity difference between successive flux nulls. Equivalently, this can be written as $\hbar/m_e=4S\Delta\nu$, since the spin frequency ν is the actual parameter that is experimentally measured. Thus, by making accurate measurements of a macroscopic area and a frequency difference, a high-precision measurement of h/m_e is possible. We note that Eq. (5) remains valid for superconducting rings thinner than the London penetration depth.

The experimentally measured value of h/m_e is subject to a relativistic mass correction, since the electrons that participate in superconductivity are on the Fermi surface and have velocities that are about 1% of the speed of light. Two theoretical analyses have been performed. In the theory of Cabrera, Gutfreund, and Little,[1] a relativistic correction to the effective vector potential is derived in the limit of a nonrelativistic rotation velocity for the lattice but which is valid for relativistic electron velocities within the lattice. They find that

$$\mathbf{A}_\omega=-(\gamma mc/e)\boldsymbol{\omega}\times\mathbf{r}\ , \tag{6}$$

where γ is defined quantum mechanically through the expectation value of the kinetic energy operator as

$$\gamma=1+\langle k_F|T|k_F\rangle/(mc^2)\ . \tag{7}$$

The average is taken over electron states within Δ, the superconducting energy gap, of the Fermi surface. For Nb, $\Delta/E_F\approx 3\times10^{-4}$, so an average over the actual Fermi surface states is a good approximation.

A second mass shift arises from the distribution of elec-

 ©1985 The American Physical Society

trons inside the atoms of a crystal. When the crystal is rotated, this distribution creates a magnetic field inside it. As a result, the total magnetic flux measured from outside the sample is smaller than the London moment flux by a factor of $1-\kappa e\Phi_{\text{Bethe}}/(mc^2)$, where Φ_{Bethe} is the inner crystal electrostatic potential originally calculated by Bethe[2] and κ is a multiplying factor which depends on the geometry of the experimental apparatus. Thus, the authors predict that the total mass shift is

$$m'=m[1+\langle T\rangle/(mc^2)-\kappa e\Phi_{\text{Bethe}}/(mc^2)] . \quad (8)$$

On the other hand, Brady[3] finds that the shift due to the potential is given by $e\langle\Phi\rangle/(mc^2)$, where $\langle\Phi\rangle$ is the expectation value of the potential energy for the electron wave functions on the Fermi surface. In addition to the electrostatic potential, he includes large exchange interaction contributions. His mass shift is given by

$$m'=m[1-W/(mc^2)] , \quad (9)$$

where the work function is $-W=\langle T\rangle-e\langle\Phi\rangle$. For niobium, Eq. (8) predicts a net mass increase of 150 ppm,[1] while Eq. (9) predicts a decrease of 10 ppm![3]

A significant systematic error can be introduced by the existence of electric charge on the rotor, which produces an additional magnetic field when rotated. The signal would be present when the ring is both normal and superconducting. This problem is dealt with in detail later in the paper.

EXPERIMENT

The superconducting ring is a 20-μm-wide, 40-nm-thick band of niobium deposited around the equator of a fused-quartz, hemispherical rotor. The cross-sectional area of the bare quartz hemisphere has been determined to an accuracy of 8 ppm.[4] Two perpendicular diameters were measured using interferometric techniques at the National Bureau of Standards at Gaithersburg. These yielded a mean diameter of 1.998 269 (8 ppm) inches for our rotor. A computer-aided Talyrond roundness measuring system was also used to ascertain that the diameter varied by no more than 2 ppm from this value.

The diameter determination was done at room temperature and has to be corrected since quartz expands by about 20 ppm on cooling to 4.2 K. In the future, high-resolution measurements of the total dimensional change of samples taken from the original rotor blanks will be made. However, until these measurements are made, the tabulated expansion coefficients, good to 5 ppm, will be used.

Niobium has been chosen as the material for the superconducting ring because it is robust and adheres well to quartz. It has a relatively high bulk transition temperature (9.2 K), so it is superconducting at 4.2 K, the temperature of liquid helium at atmospheric pressure. As a matter of fact, niobium films as thin as 4 nm are still superconducting at 4.2 K.[5] The thickness and width of the ring were chosen so that all possible cross-sectional areas bounded by the superconductor are equal to within ± 3.2 ppm.

The width and location of the niobium ring are defined by photolithographic techniques. Positive photoresist is applied to the hemisphere by dipping and is exposed by rotating the hemisphere in front of a HeCd laser beam (442-nm wavelength) focused to a 20-μm spot. A vertical translator enables the quartz equatorial plane to be positioned at precisely the same height as the laser beam.

In practice the photoresist defines the pattern, but metallic thin films form the mask for the niobium deposition. Figure 1 outlines the procedure. First, a band of 0.5-μm-thick copper and then 100-nm-thick gold is deposited on the bare substrate. The photoresist is applied, exposed, and developed, revealing a 20-μm-wide band of gold over copper [Fig. 1(a)]. Next, a solution of KI and I_2 etches both the gold and the copper, and a final etch with $FeCl_3$ undercuts the copper, leaving a gold overhang [Fig. 1(b)]. The photoresist is then removed, leaving an all-metal mask with a 20-μm-wide slit. Now the niobium thin film is deposited using an electron-beam deposition. Finally, lift-off of the mask is accomplished with $FeCl_3$. As shown in Fig. 1(c), only the 20-μm-wide niobium line remains, accurately positioned on the rotor's equator.

The h/m_e measurements are made with a cryogenic helium-gas bearing constructed entirely of fused quartz (Fig. 2). The rotor is a 5-cm-diameter sphere that has been truncated 1.39 mm above its equator. The niobium ring has been deposited around the equator. The hemisphere is supported and spun with helium gas. Two pieces of data are needed to determine $\Delta\omega=\omega_n-\omega_{n-1}$ [see Eq. (5)]: the magnetic flux and the spin speed. The data acquisition scheme is represented in Fig. 3. The flux is measured with a superconducting pick-up loop that is placed in a groove cut into the housing and is coupled to a

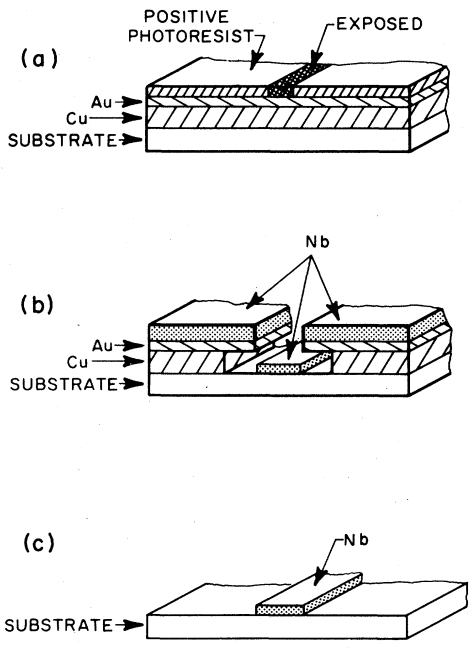

FIG. 1. The procedure used to deposit the niobium thin-film ring includes the formation of a bimetallic mask that defines the width and location of the ring.

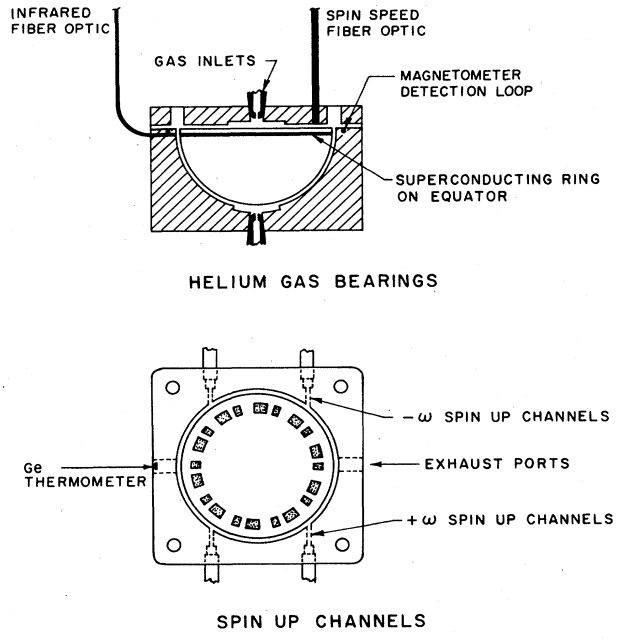

FIG. 2. Schematic of the fused-quartz, helium-gas bearing used for the h/m_e measurements.

SQUID magnetometer (superconducting quantum interference device). The rotor's spin speed is monitored using a fiber optic mounted through the cover of the housing. The intensity of the reflected light is modulated by a frosted pattern on the rotor's top surface and is analyzed to give the speed, direction, and feedback control. The average temperature of the bearing is controlled by heaters in the gas lines and a germanium thermometer located in one of the exhaust ports in the housing. In addition, the niobium ring can be rapidly modulated through its transition temperature using an infrared laser that shines directly onto the ring via another fiber optic. The ring is driven normal when a shutter in front of the infrared laser opens. As it closes and the ring enters a particular flux state, the data acquisition system is triggered, and the flux and spin speed are simultaneously measured. The flux is an average of readings taken at 50 Hz during the time in which the spin speed is being determined (typically 1 s). The entire apparatus is enclosed in a superconducting lead shield,[6] which maintains the ambient magnetic field at 5×10^{-8} G.

EXPERIMENTAL RESULTS

The frequency difference between flux nulls, $\Delta\nu$, is found by simultaneously recording the flux and spin speed for various spin speeds and flux states. A short infrared laser pulse drives the niobium ring normal every five seconds and allows a different flux state to be accessed. Figure 4 shows such data taken with a computerized data acquisition system as the spin speed was slowly ramped over $\frac{1}{4}$ Hz.

The data points (Φ,ν) can be fit to the equation

$$\nu=\Phi/S_0+n\Delta\nu+\nu_c\ , \tag{10}$$

which is merely a rewriting of Eq. (4). The intercept of

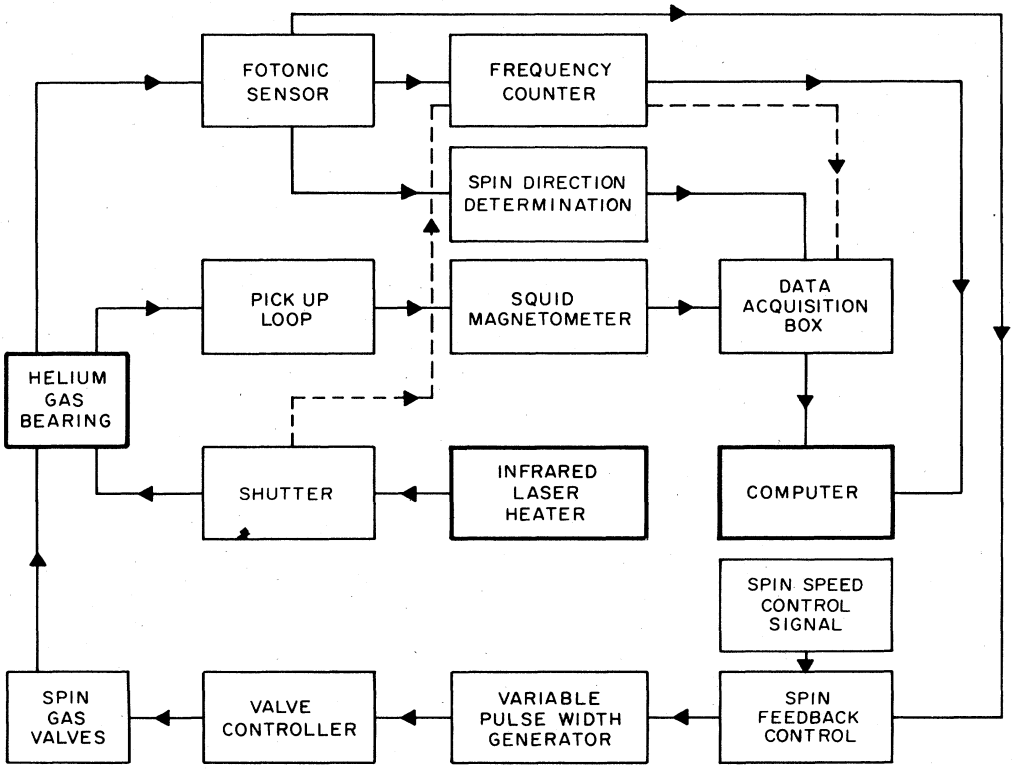

FIG. 3. Block diagram summarizing the measurement technique. The dashed lines indicate trigger signals.

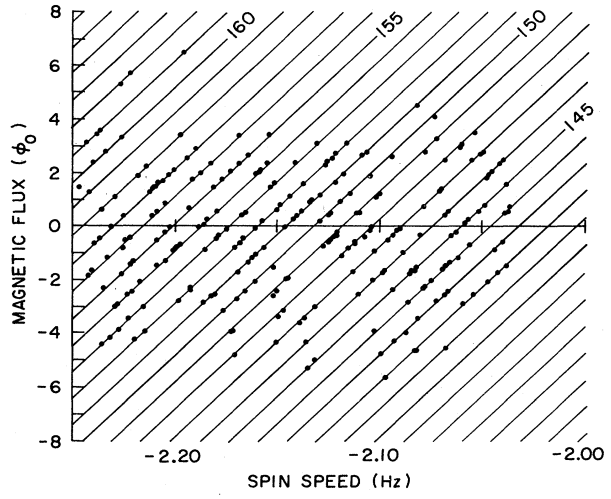

FIG. 4. High-precision data used to determine $\hbar/m_e$ obtained by slowly ramping the spin speed over $\frac{1}{4}$ Hz.

the $n=0$ line with the $\Phi=0$ axis is ν_c, a constant. S_0 is the London moment slope and is obtained separately by ramping the spin speed over several Hertz while keeping the ring in one flux state. The scatter in the data points is small enough that the lines corresponding to different quantum states n can be easily and unambiguously distinguished. The data analysis begins by finding a rough value for ν_c. Then, for the line through each data point with slope S_0, the quantum state n and the $\Phi=0$ intercept $\nu_n(=\nu-\Phi/S_0)$ are calculated. Finally, a least-squares fit to the pairs of points (n,ν_n) is performed. The slope of the best-fit line is the quantity of interest, $\Delta\nu$.

The best results are obtained by taking data at just two spin speeds separated by 10 Hz and switching between them every few minutes. This technique enables several independent values of h/m_e to be obtained in a short amount of time and is effectively a low-frequency ac measurement, reducing sensitivity to dc drift in the SQUID output. Similar measurements with the ring maintained above its transition temperature T_c detect the presence of systematic errors. The exact number of flux states between the two spin speeds still must be unambiguously determined. This is achieved by taking additional data at four spin speeds that span the same interval but are incommensurately spaced. Each intercept can be determined to about $\pm 0.5\%$ of $\Delta\nu$ for data taken in a 1-Hz bandwidth. Thus, a spin speed range of 10 Hz, or 700 nulls, gives a statistical accuracy of ≈ 10 ppm.

DISCUSSION OF THE RESULTS

When the niobium ring is in the normal state, fields are produced by Φ_{Bethe} [see Eq. (8)], the inner crystal potential, and by electric charge on the rotor. The effect of Φ_{Bethe} has been calculated and, for niobium, is expected to be no more than 30 ppm.[1] The electric charge, however, can have a much larger effect, depending on its magnitude and distribution.

We have observed a signal proportional to spin speed in the normal state, which is about 0.25% of the superconducting state signal and is in the same direction. This corresponds to the rotor being positively charged to a potential of about 1.5 kV. In addition, this normal state signal may vary by 10% on a time scale of the order of hours. A larger value of the signal corresponds to a decreased spacing of flux nulls, and vice versa. The signal size is directly proportional to spin speed over the measured range (20 Hz) and is likely to be due to a distribution of charge on the rotor.

An interesting feature of the signal is that, in addition to its dc value, there was originally a large periodic variation of the flux within each revolution of the rotor. The size of the peaks and valleys was proportional to spin speed and was roughly one flux quantum (referred to the rotating ring) at 5 Hz. In terms of the surface charge model, there must have been aggregations of both positive and negative charges on the rotor. Since the average potential was 1 kV, the local potentials must have been an order of magnitude larger.

Various attempts were made to reduce the magnitude of the charge. Grounded manganin wires were introduced into the gas lines, and this reduced the effect by a factor of 4 to its present value. Sources of alpha-particle-producing ^{241}Am were later added and positioned close to the rotor housing in the gas flow. The alpha particles ionize the helium gas, and the ions then move toward the rotor in the gas stream. However, the drift velocity of the electrons compared to that of the positive helium ions is large $[v_-/v_+=(m_+/m_-)^{1/2}]$. As a result, the electrons quickly collide with the walls and leave the gas stream before reaching the rotor. Therefore, the positive charge on the rotor was unattenuated. However, most of the ac structure of the signal disappeared with a time constant of 5 h, leaving a small residual signal which is present even when the pick-up loop is normal.

If the charge distribution is known, its effect on the measured value of $\Delta\nu$ can be calculated. A model that we have considered is that of a uniform surface charge density σ_0 over the hemisphere. With I (current), L (self-inductance), and M (mutual inductance) having subscripts P, R, S, and Q referring to the pick-up loop, ring, SQUID, and charge, respectively, we have

$$0=I_P(L_P+L_S)+I_R M_{RP}+I_Q M_{QP} , \tag{11}$$

$$n\Phi_0=4\pi(mc/e)\nu S-I_R L_R-I_Q M_{QR}-I_P M_{RP} . \tag{12}$$

The kinetic inductance L_K has been neglected, since it is much smaller than the self-inductance ($L_R/L_K\approx 700$). Solving these equations for the null flux condition, $I_P=0$, yields

$$n\Phi_0=4\pi(mc/e)\nu_n S-(M_{QR}-L_R M_{QP}/M_{RP})Q\nu_n , \tag{13}$$

with $I_Q=Q\nu_n$. We can then write the measured flux null spacing $\Delta\nu_{\text{meas}}=\nu_n-\nu_{n-1}$ as

$$\Delta\nu_{\text{meas}}=\Delta\nu_{\text{true}}[1-\epsilon(d\Phi/d\nu)_{\text{nor}}/(d\Phi/d\nu)_{\text{sc}}] , \tag{14}$$

where $(d\Phi/d\nu)_{\text{nor}}$ and $(d\Phi/d\nu)_{\text{sc}}$ measure the flux per unit frequency coupling to the pick-up loop when the ring is normal and superconducting, respectively, and

$$\epsilon=[1-M_{RP}M_{QR}/L_R M_{QP}]/[1-M_{RP}{}^2/L_R(L_P+L_S)]\ . \tag{15}$$

In general, the charge is spread out over the surface of the hemisphere. As a result, an average of the coupling constants for each annulus of charge is the quantity that comes into Eq. (14). This overall coupling constant is

$$\langle\epsilon\rangle=\int \epsilon(l)M_{PQ}(l)dI(l)\Big/\int M_{PQ}(l)dI(l)\ , \tag{16}$$

where l is a coordinate that measures position along the rotor surface and is orthogonal to the azimuthal angle.

A uniform charge distribution on the spinning rotor gives rise to a surface current density $\mathcal{J}$, which is depicted in Fig. 5(a). The linear part of the graph corresponds to the top flat of the rotor, while the sinusoidal part corresponds to the hemispherical surface. Figure 5(b) shows how such current loops couple to the pick-up loop in its present location. The mutual inductance peaks sharply in the region of the edge of the hemisphere. In the presence of a superconducting ring, however, the coupling is altered and goes to zero at the ring itself, where the charge current is completely shielded by the supercurrent. Figure 5(c) plots this shielding factor for different positions of the charge. Finally, the flux coupling to the pick-up loop per unit l is shown for the cases of a normal ring [Fig. 6(a)] and a superconducting ring [Fig. 6(b)]. The ratio of the areas under the two curves is $\langle\epsilon\rangle$, which appears in Eq. (14) as ϵ. Using estimates for the various mutual inductances, we obtain a value of 0.70 ($\pm$0.02).

In order to determine our best measured value of $\hbar/m_e$, we need to extrapolate our $\Delta\nu_{\text{meas}}$ data to find the value $\Delta\nu_{\text{true}}$. Figure 7 is a plot of the normal signal versus the

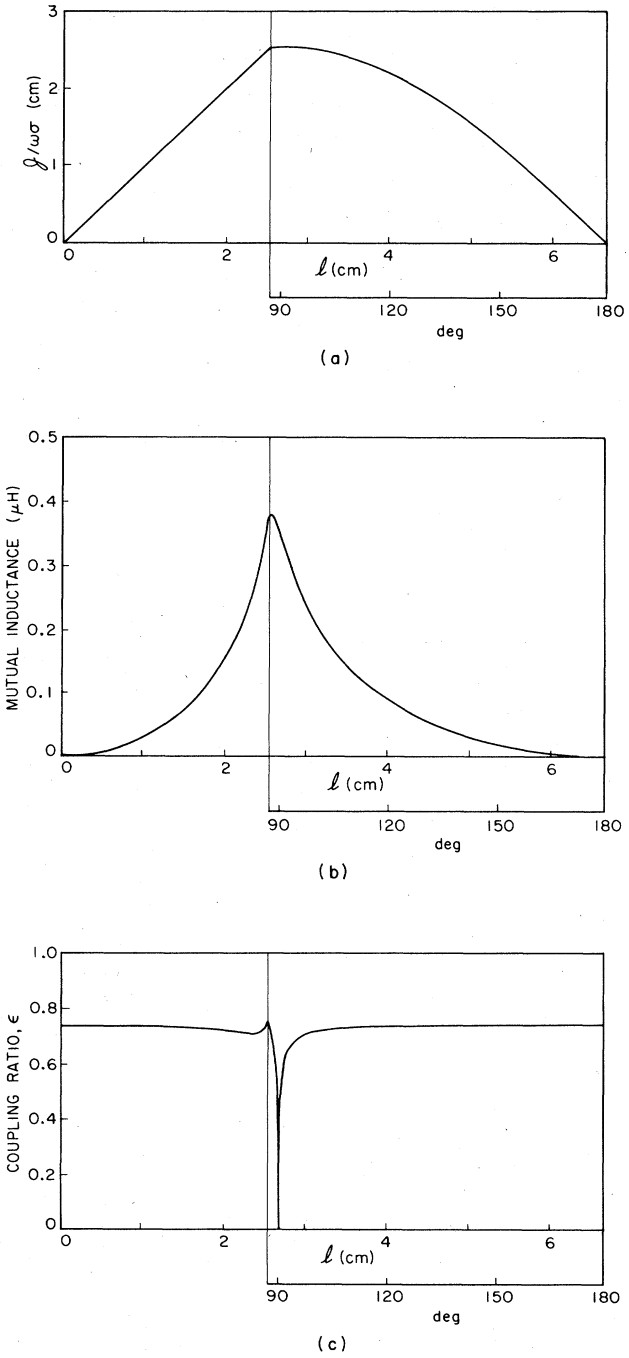

FIG. 5. Plots of (a) the surface current density around the rotor, (b) the mutual inductance between the charge and the pick-up loop when the ring is normal, and (c) the shielding factor ϵ for a uniform charge distribution.

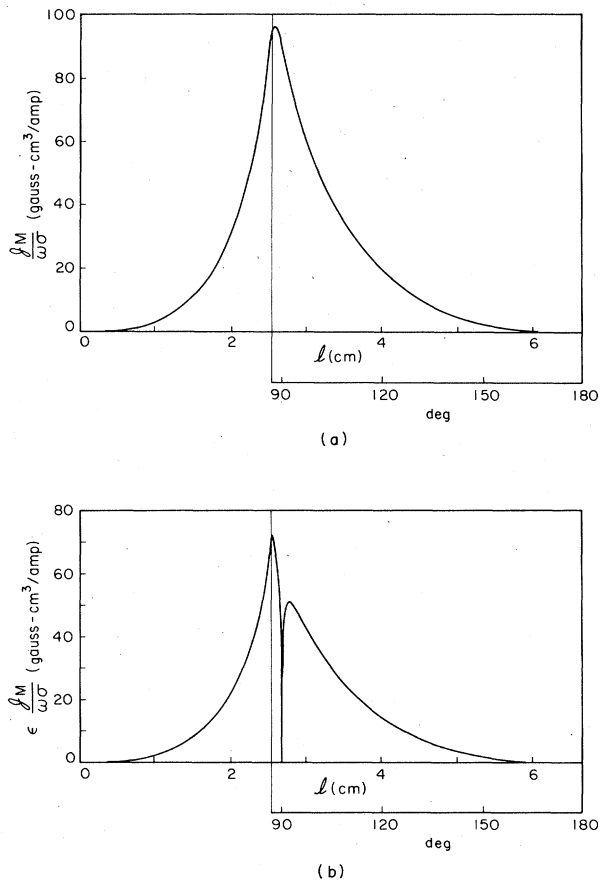

FIG. 6. Plots of the flux coupling to the pick-up loop from charge in the annulus at a position l around the hemisphere's surface when the ring is (a) normal and (b) superconducting.

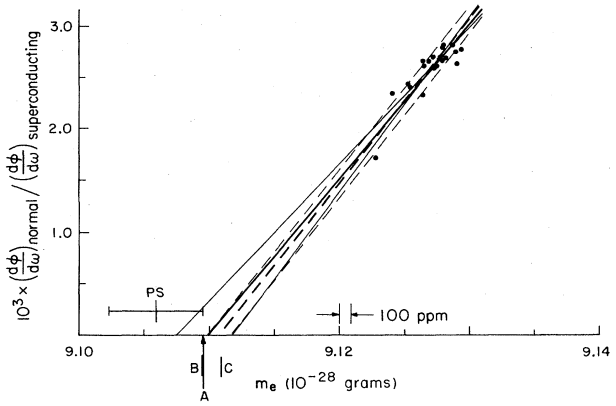

FIG. 7. Graph of the rotor charge signal versus the apparent value of m_e. Two independent estimates of the true value of m_e are obtained by extrapolating to zero charge.

value of m_e determined when that signal was present. Here we are considering Planck's constant to be the quantity in the ratio $\hbar/m_e$ that is very accurately known (it is known to 5.7 ppm).[7] So, our measurements of $\Delta\nu$ are actually yielding values of m_e for electrons in the superconductor according to the equation

$$m_e=\hbar/(4S\Delta\nu) . \tag{17}$$

One method of finding the value of m_e for zero charge is to perform a linear least-squares fit to the $(d\Phi/d\nu)_{nor}$ versus m_e data points. The bold solid line in the figure is such a fit with the finer solid lines indicating one-sigma limits. An alternative analysis is to impose a slope based on the value of ϵ calculated for a uniform charge distribution. Then, an intercept is calculated by standard statistical methods. The dotted lines in Fig. 7 show this analysis with one-sigma limits.

Several relevant, measured or calculated values for the electron mass are pointed out along the horizontal axis. The accepted value of the rest mass of an electron, m_e, is labeled "A" and is obtained from the Rydberg constant, the fine-structure constant, and the speed of light,[8] according to the equation $m_e=2hR_\infty/(\alpha^2 c)$:

$$(m_e)_A=9.109\,512\times10^{-28}\ \text{g}\ \ (5.7\ \text{ppm}) . \tag{18}$$

The values which include relativistic corrections predicted by Brady (B) and Cabrera *et al.* (C) are also indicated:

$$(m_e)_B=9.109\,421\times10^{-28}\ \text{g}$$

$$\text{(a decrease of 10 ppm)} , \tag{19}$$

$$(m_e)_C=9.110\,878\times10^{-28}\ \text{g}$$

$$\text{(an increase of 150 ppm)} . \tag{20}$$

Previously, the best reported experimental value was that of Parker and Simmonds:[9]

$$(m_e)_{PS}=9.1059\times10^{-28}\ \text{g}\ \ (400\ \text{ppm}) . \tag{21}$$

The least-squares fit gives

$$(m_e)_{LSF}=9.109\,820\times10^{-28}\ \text{g}$$

$$(+0.001\,858/-0.002\,364) . \tag{22}$$

This value is larger than the accepted value by 34 ppm, but the error bars do include B, C, and PS. If we impose a slope using $\epsilon=0.70$, then we find that

$$(m_e)_{\epsilon=0.70}=9.110\,603\times10^{-28}\ \text{g}\ (\pm0.000\,844) . \tag{23}$$

First, we note that the error in this value of m_e is about 100 ppm. This level of accuracy is four times better than that attained by Parker and Simmonds and represents the best direct measurement of m_e, the mass of an electron in superconducting niobium, and h/m_e. Second, the values of $(m_e)_{\epsilon=0.70}$ and $(m_e)_C$ are extremely close, and the error bars just exclude the accepted value and Brady's. However, since the error bars are so large, no conclusions as to the mass shift can really be formed. Nevertheless, the results slightly favor a net mass increase. We expect simple improvements to reduce the uncertainty in the measured value of m_e and allow a definitive observation of the mass shift. Further improvements in resolution to 1 ppm or better are possible and would contribute an independent datum to the knowledge of the fundamental physical constants.[10]

ACKNOWLEDGMENTS

We wish to thank Paul W. Worden for helpful ideas and discussions. This work has been supported in part by the National Science Foundation Grant No. DMR-80-26007 and by the National Bureau of Standards Precision Measurement Grant No. G8-9026.

*Permanent address: Varian Associates, Palo Alto, California.
†Permanent address: Hewlett-Packard Laboratories, Palo Alto, California.

[1]B. Cabrera, H. Gutfreund, and W. A. Little, Phys. Rev. B **25**, 6644 (1982).
[2]H. Bethe, Ann. Phys. (Leipzig) **87**, 55 (1928).
[3]R. M. Brady, J. Low Temp. Phys. **49**, 1 (1982).
[4]B. Cabrera and G. J. Siddall, Precis. Eng. **3**, 125 (1981).
[5]S. A. Wolf, J. J. Kennedy, and M. Nisenoff, J. Vac. Sci. Tech. **13**, 145 (1976).
[6]B. Cabrera and F. van Kann, Acta Astronautica **5**, 125 (1978).
[7]E. R. Cohen and B. N. Taylor, J. Phys. Chem. Ref. Data **2**, 663 (1973).
[8]E. R. Williams and P. T. Olsen, Phys. Rev. Lett. **42**, 1575 (1979).
[9]W. H. Parker and M. B. Simmonds, in Natl. Bur. Stand. (U. S.) Spec. Publ. No. 343 (U. S. G. P. O., Washington, D. C., 1970), p. 243.
[9]W. H. Parker and M. B. Simmonds, in Natl. Bur. Stand. (U.S.) Spec. Publ. No. 343 (U.S. G.P.O., Washington, D.C., 1970), p. 243.
[10]B. Cabrera, S. (Benjamin) Felch, and J. T. Anderson, in Natl. Bur. Stand. (U.S.) Spec. Publ. No. 617 (U.S. G.P.O., Washington, D.C., 1984), p. 359.